

Leveraging Superfluous Information in Contrastive Representation Learning

Xuechu Yu¹ Fangzhou Lin¹ Yun Yue¹ Ziming Zhang¹

¹Worcester Polytechnic Institute, USA

{xyu4, flin2, yyue, zzhang15}@wpi.edu

Abstract

Contrastive representation learning, which aims to learn the shared information between different views of unlabeled data by maximizing the mutual information between them, has shown its powerful competence in self-supervised learning for downstream tasks. However, recent works have demonstrated that more estimated mutual information does not guarantee better performance in different downstream tasks. Such works inspire us to conjecture that the learned representations not only maintain task-relevant information from unlabeled data but also carry task-irrelevant information which is superfluous for downstream tasks, thus leading to performance degeneration. In this paper we show that superfluous information does exist during the conventional contrastive learning framework, and further design a new objective, namely SuperInfo, to learn robust representations by a linear combination of both predictive and superfluous information. Besides, we notice that it is feasible to tune the coefficients of introduced losses to discard task-irrelevant information, while keeping partial non-shared task-relevant information according to our SuperInfo loss. We demonstrate that learning with our loss can often outperform the traditional contrastive learning approaches on image classification, object detection and instance segmentation tasks with significant improvements.

1. Introduction

Due to the huge cost in acquiring data notations, unsupervised learning has enjoyed its renaissance recently. Contrastive learning, whose goal is to learn powerful presentations for downstream tasks, has achieved promising success [56, 11, 36, 49, 21, 19, 17, 41]. Since there is no label information, contrastive learning usually estimates the mutual information between the learned representations of different views as its objective function such as SimCLR [5], and takes the learned model as a features extractor for various downstream tasks, such as image classification, object detection and instance segmentation.

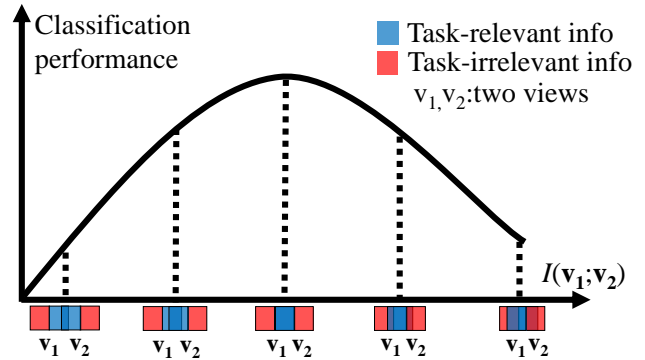


Figure 1: Classification performance vs. estimated mutual information between the two views

To understand contrastive learning, we are often based on a multi-view assumption [45, 58]: either view of the unlabeled data is (approximately) sufficient for the label information so that we can pull similar data pairs close while pushing dissimilar pairs apart to obtain the shared information of different views. From this perspective, contrastive learning aims to maximize the lower bound of the mutual information between two augmentation views of the data so that the learned presentations are useful for downstream tasks. However, some researchers find counterintuitive examples. For instance, [53, 50] argue that maximizing the lower bound of the mutual information of the learned representations can not guarantee good performance for various downstream tasks, there are other factors which can not be ignored. [50] did a series of experiments that reveals the relationship between the estimated mutual information between two augmentation views and downstream image classification performance (performance on CIFAR-10 [30] and STL-10 [8]), as shown in Figure 1, with different data augmentations, the estimated mutual information between two augmentation views becomes larger and larger, however, the downstream classification performance does not vary with the changed estimated mutual information, but rather goes up at first and then goes down.

Based on this phenomenon, we guess that the learned representations not only extract task-relevant information from the input data, but also carry task-irrelevant information which is superfluous for various downstream tasks, thus leading to performance degeneration. For the supervised learning, prior work [1] straightforwardly discards task-irrelevant information from the input data by maximizing the mutual information between the learned representation and the label, while simultaneously minimizing the mutual information between the learned representation and the input data to make the learned representation more sufficient. While in the self-supervised framework, since there is no provided label information, each view plays a supervisory role for the other one, what we pay attention to is the shared information between different augmentation views. Through detailed analysis analogously to supervised learning, we find that the mutual information between each augmentation view and its encoding is comprised of two components, task-relevant one and task-irrelevant one, further we can express each part with the notation of mutual information between different variables. As a consequence, we create a new objective function to remove task-irrelevant information while maximizing the mutual information between two different augmentation views, which can improve performance for various downstream tasks. Besides, we notice that we can tune the coefficients of introduced losses to discard task-irrelevant information, while simultaneously keeping partial non-shared task-relevant information according to different tasks. What's more, we draw a conclusion that the learned representations from our method can have a better performance than others on the downstream tasks when the multi-view redundancy is small by analyzing the Bayes Error Rate of different representations (See Section 3.3).

Overall, our contributions include:

- Based on prior works and supervised learning solutions, we excavate two independent parts, the task-relevant part and the task-irrelevant part, that make up the mutual information between each augmentation view and its encoding, and express each part with mutual information in different variables. Consequently, we design a new objective function to eliminate the task-irrelevant part.
- By applying the theory of Bayes Error Rate, we prove that our learned presentations can perform better on the downstream tasks.
- We verify the effectiveness of our method for contrastive representation learning framework by conducting image classification, object detection and instance segmentation experiments. What's more, we also run certain ablation experiments to analyze the role of the adding losses.

2. Related Work

Contrastive representation learning, one of the several self-supervised learning approaches, has significantly outperformed other approaches from recent years [44, 68, 28, 40, 13, 38, 12, 18, 66, 63, 6, 64]. With the convenience of obtaining a mass of unlabeled data, different multi-views of unlabeled data are constructed to design the specific contrastive loss to obtain a powerful learned representation, such as multiple augmentations of one image [2, 61, 46, 69, 71], different patches of one image [24, 26, 20, 18, 67, 31], text and its context [29, 34, 60, 12, 65, 47], different time slots of the same videos [70, 43, 35, 48, 4, 59], which pull similar data pairs close while push dissimilar pairs apart.

The intuition based on the contrastive idea is how to choose similar and dissimilar pairs, one feasible methodology is to maximize the shared information of different views (mutual information). Prior works [39, 5] have shown appealing performance in multiple downstream tasks according to this intuition. However, a few researchers draw some conclusions against intuition. The work by [53] argues that maximizing the tighter bound of the mutual information between different variables may lead to worse representations, the success of these promising results should be also attributed to the parametrization of the employed mutual information estimators and the choice of encoder extractor architectures. Therefore, they design several experiments to verify their hypothesis.

The work [50] demonstrates that the optimal view for contrastive representation learning is related to the given downstream tasks, meaning no need to maximize the mutual information of different views. Their InfoMin rule aims to figure out particular data augmentations to reduce the mutual information appropriately but does not find what component results in their hypothesis and does not give a general objective function, while our method considers standard augmentations (e.g., cropping, rotation, and colorization), theoretically analyzes the task-irrelevant information between different augmentations and designs a new objective function to eliminate this part. On the other hand, [52] reveals that contrastive representation learning is able to extract task-relevant information and discard task-irrelevant information with a fixed gap and quantifies the amount of information that cannot be discarded. They create a new composite self-supervised learning objective based on their analysis, but their introduced Inverse Predictive Learning seems slightly not related to their analysis logic.

What's more, [16] applies information bottleneck [51] to the multi-view learning, also aims to discard task-irrelevant information from different views during their framework, but their method is not implemented in a precise way and not tested on frequently-used datasets, our work presents a totally different and flexible objective function, and is validated on popular datasets, such as CIFAR10 [30], STL-10

[8], ImageNet [10]. A recent work [55] refutes the conclusion given by [50, 16], argues that the minimal sufficient representation contains less task-relevant information than other sufficient representations and has a non-ignorable gap with the optimal representation, which may cause performance degradation for several downstream tasks, suggesting increasing the mutual information between the input data and its encoding in the objective function. However, this adjustment maybe can bring more useful information but is also likely to introduce more noise for different downstream tasks.

3. Method

3.1. Motivation

Let us turn to supervised representation learning, the objective of supervised representation learning is to find a good representation \mathbf{z} after encoding the input data \mathbf{x} , and then use the representation \mathbf{z} for various downstream tasks, such as classification, regression. Since the label \mathbf{y} can be obtained in supervised representation learning, the training metric is usually built up with the representation \mathbf{z} and the label \mathbf{y} . What’s more, to make the representation more general and more robust, [1] applies the Information Bottleneck theory [51] to establish a new objective function, the purpose is to make the representation \mathbf{z} more sufficient for the label \mathbf{y} . We discuss the concept of sufficiency of supervised representation learning by the following definition.

Definition 1. *Sufficiency in supervised representation learning: A representation \mathbf{z} of the input data \mathbf{x} is **sufficient** for the label \mathbf{y} if and only if $I(\mathbf{x}; \mathbf{y}|\mathbf{z}) = 0$ (Where $I(\cdot)$ represents the mutual information between variables).*

According to Definition 1, we know that the learned sufficient representation \mathbf{z} contains all the information related to the label \mathbf{y} after the model properly encodes the original input data \mathbf{x} , and it may be well-performed for different evaluation tasks. Since the input data \mathbf{x} usually has high-level semantic information compared to the label \mathbf{y} , there certainly exists some information in \mathbf{x} which is irrelevant for \mathbf{y} , we can regard these as task-irrelevant (superfluous) information. By decomposing $I(\mathbf{x}; \mathbf{z})$ into two terms using the chain rule of mutual information (proof in Appendix B.1).

$$I(\mathbf{x}; \mathbf{z}) = \underbrace{I(\mathbf{y}; \mathbf{z})}_{\text{predictive information}} + \underbrace{I(\mathbf{x}; \mathbf{z}|\mathbf{y})}_{\text{superfluous information}} \quad (1)$$

The conditional mutual information $I(\mathbf{x}; \mathbf{z}|\mathbf{y})$ expresses the mutual information between \mathbf{x} and \mathbf{z} , which is task-irrelevant for \mathbf{y} , so this is superfluous. It is better to make this term as small as possible. While the other term $I(\mathbf{y}; \mathbf{z})$ represents how much task-relevant information contained in

the representation, which we want to maximize. Obviously reducing the amount of superfluous information can be done directly in supervised learning. As a consequence, [1] combines two terms $I(\mathbf{x}; \mathbf{z})$ and $I(\mathbf{y}; \mathbf{z})$ to make the model learn a more sufficient representation.

Since there is label information in the supervised setting, we can easily analyze superfluous information and useful information. As for self-supervised representation learning, there are only different augmentation views from the unlabeled data, the only useful information to be leveraged is the shared information between different views. Consider \mathbf{v}_1 and \mathbf{v}_2 as two different views of data \mathbf{x} and let \mathbf{y} be its label. Similarly \mathbf{z}_1 and \mathbf{z}_2 become representations of two different views \mathbf{v}_1 and \mathbf{v}_2 after processed by the network. Therefore, the main objective is to obtain as much shared information of two views as possible, usually maximizing the mutual information of two representations \mathbf{z}_1 and \mathbf{z}_2 ($I(\mathbf{z}_1; \mathbf{z}_2)$) is what we pay attention to. Nevertheless, like supervised representation learning, there must be some task-irrelevant (superfluous) information contained in the learned representation. Consequently we want to extract task-relevant and discard task-irrelevant information simultaneously. To formalize this we define **sufficiency** for self-supervised representation learning.

Definition 2. *Sufficiency in self-supervised representation learning: A representation \mathbf{z}_1 is **sufficient** of \mathbf{v}_1 for \mathbf{v}_2 if and only if $I(\mathbf{z}_1; \mathbf{v}_2) = I(\mathbf{v}_1; \mathbf{v}_2)$.*

Intuitively, \mathbf{z}_1 is sufficient if the amount of information in \mathbf{v}_1 about \mathbf{v}_2 is unchanged by the encoding procedure. Symmetrically, \mathbf{z}_2 is sufficient of \mathbf{v}_2 for \mathbf{v}_1 if and only if $I(\mathbf{v}_1; \mathbf{z}_2) = I(\mathbf{v}_1; \mathbf{v}_2)$.

Definition 3. *(Minimal sufficiency in self-supervised representation Learning) The sufficient representation \mathbf{z}_1^{\min} of \mathbf{v}_1 is minimal if and only if $I(\mathbf{z}_1^{\min}; \mathbf{v}_1) \leq I(\mathbf{z}_1; \mathbf{v}_1)$, $\forall \mathbf{z}_1$ that is sufficient.*

From the above definition, we can see that a sufficient representation contains exactly all the shared information between \mathbf{v}_1 and \mathbf{v}_2 . Therefore, maintaining the representations sufficient and discarding superfluous information between two views and their representations simultaneously is particularly significant. We can show the following equation by factorizing the mutual information between \mathbf{v}_1 and \mathbf{z}_1 into two terms, (similarly for \mathbf{v}_2 and \mathbf{z}_2):

$$I(\mathbf{v}_1; \mathbf{z}_1) = \underbrace{I(\mathbf{v}_2; \mathbf{z}_1)}_{\text{predictive information}} + \underbrace{I(\mathbf{v}_1; \mathbf{z}_1|\mathbf{v}_2)}_{\text{superfluous information}} \quad (2)$$

Similar to Equation 1, $I(\mathbf{v}_1; \mathbf{z}_1)$ can be decomposed into predictive information component and superfluous information component. Since $I(\mathbf{v}_2; \mathbf{z}_1)$ expresses the information between one representation and the other view, it makes a

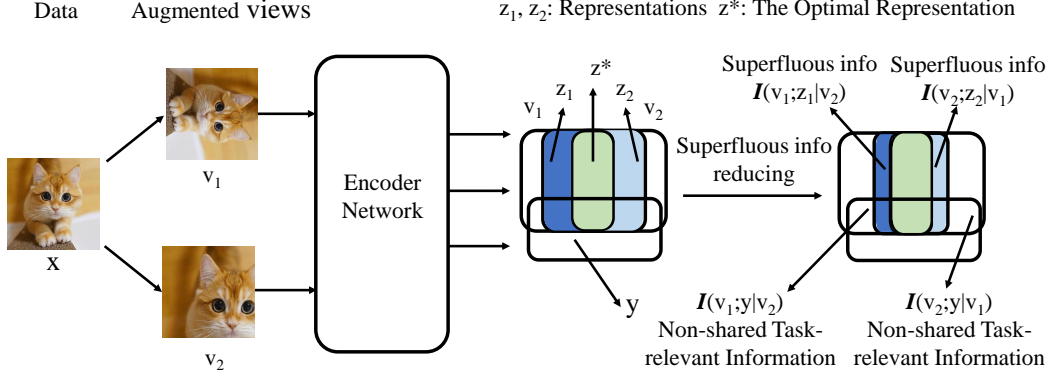


Figure 2: The information process of classical contrastive representation learning. We aim to reduce the superfluous information to make the learned representation more sufficient and robust. Meanwhile, the Non-shared task-relevant information sometimes needs to be considered.

contribution to the task-relevant information between two views. On the other hand, $I(\mathbf{v}_1; \mathbf{z}_1|\mathbf{v}_2)$ means the information contained between \mathbf{v}_1 and \mathbf{z}_1 while the view \mathbf{v}_2 has been observed, as shown in Figure 2. The larger this term, the more non-shared information between two views, so reducing (or minimizing) $I(\mathbf{v}_1; \mathbf{z}_1|\mathbf{v}_2)$ can make the learned representation more sufficient. The proof of Equation 2 can be found in appendix B.2.

3.2. SuperInfo Loss Function

Since contrastive representation learning tries to pull similar data pairs close while push dissimilar pairs apart, it maximizes the mutual information between two learned representations \mathbf{z}_1 and \mathbf{z}_2 . Based on the analysis above, it can be concluded that reducing the superfluous information may help to learn a more sufficient representation for various downstream tasks, so we can maximize the following objective function.

$$J = I(\mathbf{z}_1; \mathbf{z}_2) - \lambda_a I(\mathbf{v}_1; \mathbf{z}_1|\mathbf{v}_2) - \lambda_b I(\mathbf{v}_2; \mathbf{z}_2|\mathbf{v}_1) \quad (3)$$

Where J represents the objective function, $I(\mathbf{v}_1; \mathbf{z}_1|\mathbf{v}_2)$, $I(\mathbf{v}_2; \mathbf{z}_2|\mathbf{v}_1)$ are the superfluous information of two views analyzed above, $\lambda_i (i = a, b)$ are two Lagrangian parameters that we can tune manually.

According to the analysis in section 3.1, $I(\mathbf{v}_1; \mathbf{z}_1|\mathbf{v}_2) = I(\mathbf{v}_1; \mathbf{z}_1) - I(\mathbf{v}_2; \mathbf{z}_1)$, $I(\mathbf{v}_2; \mathbf{z}_2|\mathbf{v}_1) = I(\mathbf{v}_2; \mathbf{z}_2) - I(\mathbf{v}_1; \mathbf{z}_2)$, and since two augmentation views are symmetric to each other, we set up $\lambda_1 = \lambda_2$, $\lambda_3 = \lambda_4$ to make the objective function more general.

$$J = I(\mathbf{z}_1; \mathbf{z}_2) - \lambda_1 I(\mathbf{v}_1; \mathbf{z}_1) - \lambda_2 I(\mathbf{v}_2; \mathbf{z}_2) + \lambda_3 I(\mathbf{v}_1; \mathbf{z}_2) + \lambda_4 I(\mathbf{v}_2; \mathbf{z}_1) \quad (4)$$

What's more, since $\lambda_i (i = 1, 2)$ and $\lambda_j (i = 3, 4)$ can be set up differently based on Equation 4, we can adjust these

coefficients to discard superfluous information, while keeping partial non-shared task-relevant information according to different tasks (as shown in Figure 2, non-shared task-relevant information: $I(\mathbf{v}_1; \mathbf{y}|\mathbf{v}_2)$ and $I(\mathbf{v}_2; \mathbf{y}|\mathbf{v}_1)$), this highlights another advantage of our objective function.

We want to maximize the objective function J , but it is intractable to deal with mutual information expressions, therefore, we have to maximize the lower bound of J for second best. We first consider the term $I(\mathbf{v}_i; \mathbf{z}_i) (i = 1, 2)$,

$$\begin{aligned} I(\mathbf{v}_i; \mathbf{z}_i) &= \iint d\mathbf{v}_i d\mathbf{z}_i p(\mathbf{v}_i, \mathbf{z}_i) \log \frac{p(\mathbf{z}_i|\mathbf{v}_i)}{p(\mathbf{z}_i)} \\ &= \iint d\mathbf{v}_i d\mathbf{z}_i p(\mathbf{v}_i, \mathbf{z}_i) \log p(\mathbf{z}_i|\mathbf{v}_i) - \int d\mathbf{z}_i p(\mathbf{z}_i) \log p(\mathbf{z}_i) \end{aligned} \quad (5)$$

In general, computing the marginal distribution of \mathbf{z}_i might be difficult. Make $r(\mathbf{z}_i)$ is a variational approximation to this marginal, since $\mathbf{KL}[p(\mathbf{z}_i), r(\mathbf{z}_i)] \geq 0$, we can get the following upper bound of $I(\mathbf{v}_i; \mathbf{z}_i)$, in Equation 6, we further assume the encoder process follows the Gaussian distribution, $p(\mathbf{z}_i|\mathbf{v}_i) = \mathcal{N}(\mathbf{z}_i; f_i(\mathbf{v}_i), \sigma_i^2 I)$ and the variational approximation $r(\mathbf{z}_i) = \mathcal{N}(\mathbf{0}, I)$, so we can handle the **KL** divergence terms(full proof in Appendix C.1).

$$I(\mathbf{v}_i; \mathbf{z}_i) \leq \iint d\mathbf{v}_i d\mathbf{z}_i p(\mathbf{v}_i, \mathbf{z}_i) \log \frac{p(\mathbf{z}_i|\mathbf{v}_i)}{r(\mathbf{z}_i)} \quad (6)$$

On the other hand, we need the lower bound of the positive terms $I(\mathbf{v}_1; \mathbf{z}_2)$ and $I(\mathbf{v}_2; \mathbf{z}_1)$, take $I(\mathbf{v}_1; \mathbf{z}_2)$ as the example. Using the relationship between mutual information expression and entropy expression $I(\mathbf{v}_1; \mathbf{z}_2) = H(\mathbf{v}_1) - H(\mathbf{v}_1|\mathbf{z}_2)$, where $H(\mathbf{v}_1)$ is a constant given the augmentation view, so we only need to maximize $-H(\mathbf{v}_1|\mathbf{z}_2) = \mathbb{E}_{p(\mathbf{v}_1, \mathbf{z}_2)}[\log p(\mathbf{v}_1|\mathbf{z}_2)]$. Assuming $q(\mathbf{v}_1|\mathbf{z}_2)$ is the variational approximation to $p(\mathbf{v}_1|\mathbf{z}_2)$ in order to deal with the intractability of this conditional distribution, we have the

lower bound of $I(\mathbf{v}_1; \mathbf{z}_2)$, in Equation 7. Further we suppose $q(\mathbf{v}_1 | \mathbf{z}_2) = \mathcal{N}(\mathbf{v}_1; h_1(\mathbf{z}_2), \sigma_3^2 I)$, where h_1 maps \mathbf{z}_2 to \mathbf{v}_1 which we can use an compact **deConvNet** for realization, thus, we can estimate $\mathbb{E}_{p(\mathbf{v}_1, \mathbf{z}_2)}[\log q(\mathbf{v}_1 | \mathbf{z}_2)]$. The complete proof can be found in Appendix C.2 (similar to $I(\mathbf{v}_2; \mathbf{z}_1)$).

$$I(\mathbf{v}_1; \mathbf{z}_2) \geq \mathbb{E}_{p(\mathbf{v}_1, \mathbf{z}_2)}[\log p(\mathbf{v}_1 | \mathbf{z}_2)] \quad (7)$$

To sum up, we are able to maximize the lower bound of the objective function, so the loss function L is listed in Equation 8, where $I(\mathbf{z}_1; \mathbf{z}_2)$ can be estimated by MINE estimator [3], JS divergence estimator [24], InfoNCE loss [39]. We name our loss ‘‘SuperInfo’’ loss, the algorithm is on the right.

$$L = -I(\mathbf{z}_1; \mathbf{z}_2) + \sum_{i=1}^2 \lambda_i \mathbf{KL}[p(\mathbf{z}_i | \mathbf{v}_i), r(\mathbf{z}_i)] \\ - \lambda_3 \mathbb{E}_{p(\mathbf{v}_1, \mathbf{z}_2)}[\log q(\mathbf{v}_1 | \mathbf{z}_2)] - \lambda_4 \mathbb{E}_{p(\mathbf{v}_2, \mathbf{z}_1)}[\log q(\mathbf{v}_2 | \mathbf{z}_1)] \quad (8)$$

3.3. Bayes Error Rate of Contrastive Learning Representations

In this subsection, we apply Bayes error rate [15] to analyze the irreducible error of self-supervised contrastive learning representations. Suppose the downstream task is classification and T represents the categorical variable. It represents the smallest acceptable error when estimating the correct label given any learned representations. Basically, let P_e be the Bayes error rate of arbitrary self-supervised learning representations \mathbf{z}_1 and \hat{T} be the prediction for T from our classification model. According to [15], $P_e = 1 - \mathbb{E}_{p(\mathbf{z}_1)}[\max_{t \in T} p(\hat{T} = t | \mathbf{z}_1)]$, so $0 \leq P_e \leq 1 - 1/|T|$ where $|T|$ is the cardinality of T . We define a threshold function $\Gamma(x) = \min\{\max\{x, 0\}, 1 - 1/|T|\}$ for better analysis. [55] has proved the following theory (Full proof can be found in this paper).

Theorem 1. [55] (*Bayes Error Rate of Representations*) For arbitrary self-supervised learning representation \mathbf{z}_1 , its Bayes error rate $P_e = \Gamma(\bar{P}_e)$ with

$$\bar{P}_e \leq 1 - \exp[-(H(T) - I(\mathbf{z}_1, T | \mathbf{v}_2) - I(\mathbf{z}_1, \mathbf{v}_2, T))] \quad (9)$$

Thus, when the learned representation \mathbf{z}_1^{suf} is sufficient, its Bayes error rate $P_e^{suf} = \Gamma(\bar{P}_e^{suf})$ with

$$\bar{P}_e^{suf} \leq 1 - \exp[-(H(T) - I(\mathbf{z}_1^{suf}, T | \mathbf{v}_2) - I(\mathbf{v}_1, \mathbf{v}_2, T))] \quad (10)$$

Further for the minimal sufficient representation \mathbf{z}_1^{min} , its Bayes error rate $P_e^{min} = \Gamma(\bar{P}_e^{min})$ with

$$\bar{P}_e^{min} \leq 1 - \exp[-(H(T) - I(\mathbf{v}_1, \mathbf{v}_2, T))] \quad (11)$$

Algorithm 1 Training with SuperInfo

input: batch size N , temperature τ , hyperparameter $\lambda_i (i = 1, 2, 3, 4)$, encoder network f , g , data transformation \mathcal{T} , sampling network q_μ (MLP), q_σ (MLP), reconstruct network r (deConvNet).

for sampled minibatch $\{\mathbf{x}_k\}_{k=1}^N$ **do**

for all $k \in \{1, \dots, N\}$ **do**

$t \sim \mathcal{T}, t' \sim \mathcal{T}$

 // two augmentations

$\tilde{\mathbf{x}}_{2k-1} = t(\mathbf{x}_k), \tilde{\mathbf{x}}_{2k} = t'(\mathbf{x}_k)$

 // networks process to get the representation

$\mathbf{h}_{2k-1} = f(\tilde{\mathbf{x}}_{2k-1}), \mathbf{h}_{2k} = f(\tilde{\mathbf{x}}_{2k})$

 // obtain μ and σ of assumed Gaussian distribution

$\boldsymbol{\mu}_{2k-1} = q_\mu(\mathbf{h}_{2k-1}), \boldsymbol{\mu}_{2k} = q_\mu(\mathbf{h}_{2k})$

$\boldsymbol{\sigma}_{2k-1} = q_\sigma(\mathbf{h}_{2k-1}), \boldsymbol{\sigma}_{2k} = q_\sigma(\mathbf{h}_{2k})$

 // reconstruct input from the representations

$\mathbf{x}'_{2k-1} = r(\mathbf{h}_{2k-1}), \mathbf{x}'_{2k} = r(\mathbf{h}_{2k})$

 // get the projection after the projection head

$\mathbf{z}_{2k-1} = g(\mathbf{h}_{2k-1}), \mathbf{z}_{2k} = g(\mathbf{h}_{2k})$

end for

for all $i \in \{1, \dots, 2N\}$ and $j \in \{1, \dots, 2N\}$ **do**

 1) apply method to estimate $-I(\mathbf{z}_i; \mathbf{z}_j)$

 2) calculate Gaussian distribution KL divergence

 using $\boldsymbol{\mu}_i, \boldsymbol{\mu}_j, \boldsymbol{\sigma}_i, \boldsymbol{\sigma}_j$

 3) calculate distance $\mathbf{Dis}(\mathbf{x}_i, \mathbf{x}'_i)$ and $\mathbf{Dis}(\mathbf{x}_j, \mathbf{x}'_j)$

end for

$$L_{CL} = \frac{1}{2N} \sum_{i,j=1}^{2N} (-I(\mathbf{z}_i; \mathbf{z}_j))$$

$$L_{KL} = \frac{1}{2N} \sum_{i,j=1}^{2N} (\lambda_1 KL(\boldsymbol{\mu}_i, \boldsymbol{\sigma}_i) + \lambda_2 KL(\boldsymbol{\mu}_j, \boldsymbol{\sigma}_j))$$

$$L_{RE} = \frac{1}{2N} \sum_{i,j=1}^{2N} (-\lambda_3 \mathbf{Dis}(\mathbf{x}_i, \mathbf{x}'_i) - \lambda_4 \mathbf{Dis}(\mathbf{x}_j, \mathbf{x}'_j))$$

$$\mathcal{L} = L_{CL} + L_{KL} + L_{RE}$$

 update networks f and g to minimize \mathcal{L}

end for

output encoder network $f(\cdot)$

Observing Equation 10 and 11, we have that P_e^{min} has a larger upper bound than P_e^{suf} since $I(\mathbf{z}_1^{suf}, T | \mathbf{v}_2) \geq 0$. Therefore, [55] argues increase $I(\mathbf{v}_1; \mathbf{z}_1)$ to introduce more information that is relevant to different downstream tasks, but it also brings certain ‘‘noise’’, while we can adjust the coefficients of Equation 4 to keep partial non-shared task-relevant information according to different tasks. This improvement provides us with a trade-off between the sufficiency of the learned representations and its Bayes error rate.

4. Experiments

In this section, we verify our new SuperInfo loss through several experiments. Based on our experimental results, we

Table 1: Linear evaluation accuracy (%) from CIFAR10 and STL-10 with the standard ResNet-18 backbone network.

Method	CIFAR10	DTD	MNIST	FaMNIST	VGGFlower	CUBirds	TrafficSigns
CMC [49]	85.06	28.77	96.48	87.91	41.67	8.19	91.62
BYOL [19]	85.64	31.22	97.15	88.92	40.90	8.84	92.17
SimCLR [5]	85.70	29.52	97.03	88.36	42.81	8.87	92.41
MIB [16]	85.68	32.66	97.57	89.31	44.79	8.95	93.36
SSL Composite [52]	85.90	33.25	97.72	89.72	51.82	9.88	94.58
InfoCL+RC [55]	85.78	33.67	97.99	90.31	54.16	10.89	95.84
InfoCL+LBE [55]	85.45	34.52	97.94	89.26	54.10	10.60	94.96
SuperInfo(ours)	86.38	34.86	98.11	91.42	53.79	12.16	96.06
Method	STL-10	DTD	MNIST	FaMNIST	VGGFlower	CUBirds	TrafficSigns
CMC [49]	78.03	37.99	94.07	86.92	48.71	7.52	75.89
BYOL [19]	80.83	40.05	94.45	87.23	49.41	8.54	77.54
SimCLR [5]	78.86	39.41	95.00	87.31	49.41	8.34	80.25
MIB [16]	79.09	40.91	96.78	88.47	52.65	9.88	85.48
SSL Composite [52]	79.56	42.88	97.04	89.82	57.61	10.86	94.56
InfoCL+RC [55]	79.21	41.81	97.48	89.98	60.46	10.03	94.73
InfoCL+LBE [55]	80.17	42.07	97.04	88.68	58.51	10.11	87.77
SuperInfo(ours)	82.24	44.15	97.85	90.69	57.93	12.87	94.64

Table 2: Linear evaluation accuracy (%) from ImageNet with the standard ResNet-50 backbone network.

Method	ImageNet	CIFAR10	CIFAR100	DTD	VGGFlower	CUBirds	TrafficSigns
CMC [49]	58.87	80.96	58.61	68.96	92.85	35.26	95.03
BYOL [19]	61.55	82.95	61.65	70.86	94.08	36.97	95.92
SimCLR [5]	61.01	82.30	59.86	70.16	93.52	36.49	95.27
MIB [16]	61.11	82.68	60.79	70.91	93.66	37.09	96.07
SSL Composite [52]	61.62	82.89	61.97	71.08	95.08	37.71	96.61
InfoCL+RC [55]	61.60	83.30	63.56	71.22	94.53	37.42	96.47
InfoCL+LBE [55]	61.37	83.20	61.99	70.95	94.34	37.78	95.99
SuperInfo(ours)	62.24	83.89	64.08	72.37	94.96	39.36	96.90

also provide specific analysis.

4.1. Verifying the Role of Superfluous Information

We apply the SuperInfo loss to classical contrastive representation learning framework, and pre-train the model on CIFAR10 [30], STL-10 [8], and ImageNet [10], the learned representation is used for different downstream tasks: classification, detection and segmentation. We choose previous work as the baselines: CMC [49], SimCLR [5], BYOL [19], MIB [16], Composite SSL [52], InfoCL [55] (There are several baselines that are not tested on the three datasets, we try our best to get the results).

Data augmentations. We use the similar set of image augmentations as in SimCLR [5]. For CIFAR10 [30] and STL-10 [8], random cropping, flip and random color distortion are applied, and for ImageNet [10], a random patch of the image is selected and resized to 224×224 with a random horizontal flip, followed by a color distortion, consisting of a random sequence of brightness, contrast, saturation, hue adjustments, and an optional grayscale conversion. Finally Gaussian blur and solarization are applied to the patches.

Architecture. We train ResNet-18 [23] for CIFAR10 [30],

STL-10 [8] whose output is a 512-dim vector, then we apply an MLP to get a 128-dim vector that can be used for $I(\mathbf{z}_1; \mathbf{z}_2)$ estimation. For ImageNet [10], we use ResNet-50 [23] whose output is a 2048-dim vector, then we apply an MLP to get the projector. The output of the ResNet is used as the representation for downstream tasks.

Pretrain. We apply the Adam optimizer [27] with the learning rate $3e-4$ to train the ResNet-18 [23] backbone on CIFAR10 [30] and STL-10 [8] with batch size 256 for 200 epochs, we set $\lambda_1 = \lambda_2 = 0.01$, $\lambda_3 = \lambda_4 = 0.1$. For ImageNet [10], we use the LARS optimizer [62] to train the ResNet-50 [23] backbone with batch size 1024 for 200 epochs, we set the base learning rate to 0.3, scaled linearly with the batch size ($\text{LearningRate} = 0.3 \times \text{BatchSize}/256$). In addition, we use a global weight decay parameter of 1.5×10^{-6} while excluding the biases and batch normalization parameters from both LARS adaptation and weight decay, we set $\lambda_1 = \lambda_2 = 0.01$, $\lambda_3 = \lambda_4 = 0.1$. While estimating the term $I(\mathbf{z}_1; \mathbf{z}_2)$, we choose InfoNce method.

Evaluation. We first evaluate the learned representation from CIFAR10 [30], STL-10 [8], ImageNet [10] by training a linear classifier on top of the frozen backbone, fol-

Method	CIFAR10	DTD	MNIST	FaMNIST	VGGFlower	CUBirds	TrafficSigns
SuperInfo	86.38	34.86	98.11	91.42	53.79	12.16	96.06
SuperInfo($\lambda_1 = \lambda_2 = 0, \lambda_3 = \lambda_4 = 0.1$)	86.51	34.47	97.99	90.77	53.19	11.88	95.64
SuperInfo($\lambda_1 = \lambda_2 = 0.01, \lambda_3 = \lambda_4 = 0$)	86.29	32.69	97.22	89.09	50.17	9.89	94.13
Method	STL-10	DTD	MNIST	FaMNIST	VGGFlower	CUBirds	TrafficSigns
SuperInfo	82.24	44.15	97.85	90.69	57.93	12.87	94.64
SuperInfo($\lambda_1 = \lambda_2 = 0, \lambda_3 = \lambda_4 = 0.1$)	82.43	43.16	97.46	89.87	57.16	12.61	94.19
SuperInfo($\lambda_1 = \lambda_2 = 0.01, \lambda_3 = \lambda_4 = 0$)	82.11	42.19	97.18	88.64	56.91	10.01	93.86

Table 3: Linear evaluation accuracy with different loss terms(%) from CIFAR10 and STL-10 with the standard ResNet-18 backbone (the best result in bold)

lowing the procedure described in [5, 21, 49, 19]. The linear classifier is comprised of a fully-connected layer followed by softmax trained with the SGD optimizer for 100 epochs. The linear evaluation is conducted on other classification datasets: DTD [7], MNIST [32], FashionMNIST [57], CUBirds [54], VGGFlower [37], Traffic Signs [25] and CIFAR100 [30], performance is reported using standard metrics for each benchmark. We report the results in Table 1 and Table 2.

We can see that SuperInfo beats all previous methods on CIFAR10, STL and ImageNet, improving the state-of-the-art results by $\sim 1\%$ to 2% , what’s more, the downstream classification results show that SuperInfo outperforms other methods on 6 of the 8 benchmarks, providing only slightly worse performance on VGGFlower and TrafficSigns compared to InfoCL method.

Other vision tasks. We evaluate our representation on different tasks, object detection and instance segmentation. With this evaluation, we know whether SuperInfo’s representation generalizes beyond classification tasks.

PASCAL VOC object detection [14]. The model is Faster R-CNN [42] with a backbone of R50-C4 [22] with BN tuned. We fine-tune all methods end-to-end, The image scale is [480, 800] pixels during training and 800 at inference. The same setup is used for all methods, We evaluate the default VOC metric of AP₅₀ (i.e., IoU threshold is 50%) and the more stringent metrics of COCO-style AP and AP₇₅. Evaluation is on the VOC test₂₀₀₇ set. Table 4 shows the results fine-tuned on trainval₂₀₀₇ ($\sim 16.5k$ images). SuperInfo is better than all previous counterparts: up to **+0.9 AP₅₀**, **+1.6 AP**, and **+2.2 AP₇₅**.

COCO object detection and segmentation [33]. The detector is Mask R-CNN [22] with the R50-C4 backbone [22], with BN tuned. The image scale is in [640, 800] pixels during training and is 800 at inference. We fine-tune all methods on the train₂₀₁₇ set ($\sim 118k$ images) and evaluate on val₂₀₁₇, following the default $2\times$ schedule. We report the results in Table 5. According the results, we can see that SuperInfo achieves the state-of-the-art results based on the settings above.

Model	AP	AP ₅₀	AP ₇₅
random initialization	34.8	63.1	35.2
CMC	45.1	75.9	47.1
BYOL	47.1	77.5	48.9
SimCLR	45.5	76.2	47.5
MIB	46.6	77.1	48.5
SSL Composite	47.5	77.8	49.9
InfoCL+RC	48.1	78.0	50.9
InfoCL+LBE	47.4	77.8	49.7
SuperInfo	49.7 (+1.6)	79.1 (+1.1)	53.1 (+2.2)

Table 4: Comparison with previous methods on object detection on PASCAL VOC, fine-tuned on trainval₂₀₀₇ and evaluated on test₂₀₀₇. In the brackets are the gaps to the previous best results.

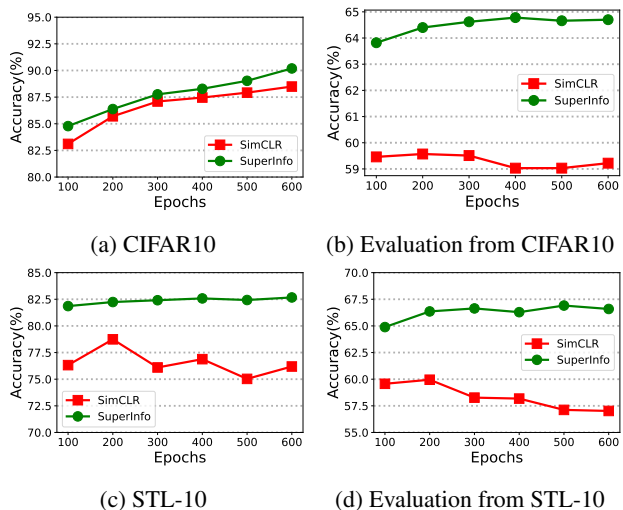


Figure 3: Classification evaluation accuracy on CIFAR10 and STL-10, and other transfer datasets (Average Accuracy) with training epochs.

4.2. Ablation Study

Analyzing the role of the added loss terms. We introduce two new losses into the classical contrastive representation learning loss to make the learned representation more ro-

Model	AP^{bb}	AP_{50}^{bb}	AP_{75}^{bb}
random initialization	35.6	54.6	38.2
CMC	38.0	58.0	41.7
BYOL	39.0	58.8	42.2
SimCLR	38.6	58.5	41.8
MIB	38.9	58.7	42.2
SSL Composite	39.1	58.8	42.3
InfoCL+RC	39.3	59.0	42.6
InfoCL+LBE	39.0	58.7	42.3
SuperInfo	39.9 (+0.6)	59.6 (+0.6)	43.4 (+0.8)

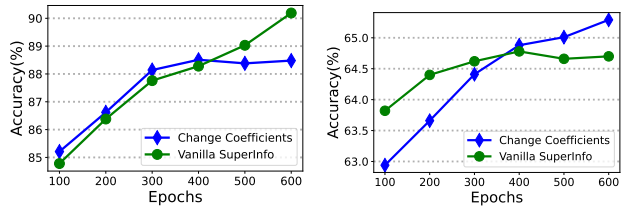
(a) Object detection on COCO

Model	AP^{mk}	AP_{50}^{mk}	AP_{75}^{mk}
random initialization	31.4	51.5	33.5
CMC	33.1	54.8	35.0
BYOL	34.1	55.4	36.3
SimCLR	33.9	55.2	36.0
MIB	34.1	55.3	36.3
SSL Composite	34.3	55.5	36.5
InfoCL+RC	34.5	55.7	36.6
InfoCL+LBE	34.2	55.4	36.4
SuperInfo	35.5 (+1.0)	56.6 (+0.9)	37.8 (+1.2)

(b) Instance segmentation on COCO

Table 5: **Object detection and instance segmentation fine-tuned on COCO:** bounding-box AP (AP^{bb}) and mask AP (AP^{mk}) evaluated on `val2017`. In the brackets are the gaps to the previous best results. In green are the gaps of at least **+0.5** point.

bust and sufficient. Further by analyzing the information flow in the framework (Figure 2), we can adjust the coefficients λ_i to discard superfluous information, while keeping partial non-shared task-relevant information according to different tasks since the term $(I(\mathbf{v}_1; \mathbf{z}_2), I(\mathbf{v}_2; \mathbf{z}_1))$ introduces certain information from different views which may make contribution to some downstream tasks. Therefore, we conduct the classification experiments (including downstream classification) of only adding the terms, $I(\mathbf{v}_1; \mathbf{z}_1), I(\mathbf{v}_2; \mathbf{z}_2)$ ($\lambda_3 = \lambda_4 = 0$) or only adding another terms, $I(\mathbf{v}_1; \mathbf{z}_2), I(\mathbf{v}_2; \mathbf{z}_1)$ ($\lambda_1 = \lambda_2 = 0$) to see whether there are apparent different performances with the original SuperInfo ($\lambda_1 = \lambda_2 = 0.01, \lambda_3 = \lambda_4 = 0.1$). Following the same setting in section 4.1, we just train the model on CIFAR10 and STL-10 by changing λ_i and apply linear evaluation protocol to other classification datasets. We report the results in Table 3. It can be clearly seen that the accuracy on the source dataset (CIFAR10 and STL-10) can achieve the similar level compared to original SuperInfo while only adding $I(\mathbf{v}_1; \mathbf{z}_1)$ and $I(\mathbf{v}_2; \mathbf{z}_2)$ since this change can discard superfluous information, but the downstream classification performance gets worse to a certain extent because several non-shared task-relevant information does not keep. On the other hand, only adding $I(\mathbf{v}_1; \mathbf{z}_2)$ and $I(\mathbf{v}_2; \mathbf{z}_1)$ is better than original SuperInfo on the source dataset (CIFAR10 and STL-10), but can not beat original SuperInfo on



(a) CIFAR10

(b) Evaluation from CIFAR10

Figure 4: Classification evaluation accuracy on CIFAR10 and STL-10, and other transfer datasets (Average Accuracy) with training epochs: Vanilla SuperInfo vs. Changing coefficients of SuperInfo

transfer datasets, which means only introducing non-shared task-relevant information may bring certain noise, leading to the phenomenon of over-fitting on transfer datasets.

Training with more epochs. We train all models for 200 epochs during all above experiments. Further we train our model for 100, 200, 300, 400, 500, 600 epochs to analyze SuperInfo’s behavior under different training epochs, compared to vanilla SimCLR. The results are listed in Figure 3. According to the above figure, we find that the downstream classification accuracy does not become better with more training epochs, even decreases in the middle period since the learned representations in contrastive representation learning are able to get more close to the minimal sufficient representation which only contains the shared information between different views with more training epochs and the minimal sufficient representation may have the risk of over-fitting on the transfer datasets. This phenomenon is consistent with the conclusion in [55]. What’s more, SuperInfo does bring significant improvements compared to vanilla SimCLR on the transfer datasets under every training epochs. On the other hand, we change the coefficients ($\lambda_1 = \lambda_2 = 0.005, \lambda_3 = \lambda_4 = 0.5$) compared to vanilla SuperInfo, training the model on CIFAR10 and evaluating the model on other transfer datasets. The results are reported in Figure 4. As shown in 4(b), the classification accuracy increases stably with the training epochs, however, the performance on the source dataset (CIFAR10) does not keep the pace with it. This phenomenon shows there really exists a trade-off of the performance on source dataset and on other transfer datasets with respect to the coefficients.

5. Conclusion and Discussion

In this work, we deeply analyze the reason why more estimated mutual information between two different views in contrastive representation learning does not guarantee great performance in various downstream tasks and design a new objective function to discards task-irrelevant information, while keeping some non-shared task-relevant information.

The effectiveness of our method are verified by several experiments.

There are a few limitations during our presentation. (1) It is still troublesome to determine the coefficients λ_i of the loss function since they apparently influence the performance, so far we have to tune them manually. (2) Due to our limited computing resources, we can not compare our best results to other methods under the condition of 4096 batch size or larger, and more training epochs, however, a series of better outcomes indicate our method can make contribution to classical contrastive representation learning framework.

References

- [1] Alexander A Alemi, Ian Fischer, Joshua V Dillon, and Kevin Murphy. Deep variational information bottleneck. In *ICLR*, 2017.
- [2] Philip Bachman, R Devon Hjelm, and William Buchwalter. Learning representations by maximizing mutual information across views. *Advances in neural information processing systems*, 32, 2019.
- [3] Mohamed Ishmael Belghazi, Aristide Baratin, Sai Rajeswar, Sherjil Ozair, Yoshua Bengio, Aaron Courville, and R Devon Hjelm. Mine: mutual information neural estimation. *arXiv preprint arXiv:1801.04062*, 2018.
- [4] Minghao Chen, Fangyun Wei, Chong Li, and Deng Cai. Frame-wise action representations for long videos via sequence contrastive learning. In *Proceedings of the IEEE/CVF Conference on Computer Vision and Pattern Recognition*, pages 13801–13810, 2022.
- [5] Ting Chen, Simon Kornblith, Mohammad Norouzi, and Geoffrey Hinton. A simple framework for contrastive learning of visual representations. In *ICML*, 2020.
- [6] Xinlei Chen and Kaiming He. Exploring simple siamese representation learning. In *Proceedings of the IEEE/CVF conference on computer vision and pattern recognition*, pages 15750–15758, 2021.
- [7] Mircea Cimpoi, Subhransu Maji, Iasonas Kokkinos, Sammy Mohamed, and Andrea Vedaldi. Describing textures in the wild. In *Proceedings of the IEEE conference on computer vision and pattern recognition*, pages 3606–3613, 2014.
- [8] Adam Coates, Andrew Ng, and Honglak Lee. An analysis of single-layer networks in unsupervised feature learning. In *Proceedings of the fourteenth international conference on artificial intelligence and statistics*, pages 215–223. JMLR Workshop and Conference Proceedings, 2011.
- [9] Thomas M Cover, Joy A Thomas, et al. Entropy, relative entropy and mutual information. *Elements of information theory*, 1991.
- [10] Jia Deng, Wei Dong, Richard Socher, Li-Jia Li, Kai Li, and Li Fei-Fei. Imagenet: A large-scale hierarchical image database. In *2009 IEEE conference on computer vision and pattern recognition*, pages 248–255. Ieee, 2009.
- [11] Jacob Devlin, Ming-Wei Chang, Kenton Lee, and Kristina Toutanova. Bert: Pre-training of deep bidirectional transformers for language understanding. *arXiv preprint arXiv:1810.04805*, 2018.
- [12] Carl Doersch, Abhinav Gupta, and Alexei A Efros. Unsupervised visual representation learning by context prediction. In *Proceedings of the IEEE international conference on computer vision*, pages 1422–1430, 2015.
- [13] Jeff Donahue and Karen Simonyan. Large scale adversarial representation learning. *Advances in neural information processing systems*, 32, 2019.
- [14] Mark Everingham, Luc Van Gool, Christopher KI Williams, John Winn, and Andrew Zisserman. The pascal visual object classes (voc) challenge. *International journal of computer vision*, 88:303–308, 2009.
- [15] Meir Feder and Neri Merhav. Relations between entropy and error probability. *IEEE Transactions on Information theory*, 40(1):259–266, 1994.
- [16] Marco Federici, Anjan Dutta, Patrick Forr’e, Nate Kushman, and Zeynep Akata. Learning robust representations via multi-view information bottleneck. In *ICLR*, 2020.
- [17] Tianyu Gao, Xingcheng Yao, and Danqi Chen. Simcse: Simple contrastive learning of sentence embeddings. *arXiv preprint arXiv:2104.08821*, 2021.
- [18] Spyros Gidaris, Praveer Singh, and Nikos Komodakis. Unsupervised representation learning by predicting image rotations. *arXiv preprint arXiv:1803.07728*, 2018.
- [19] Jean-Bastien Grill, Florian Strub, Florent Altché, Corentin Tallec, Pierre Richemond, Elena Buchatskaya, Carl Doersch, Bernardo Avila Pires, Zhaohan Guo, Mohammad Gheshlaghi Azar, et al. Bootstrap your own latent—a new approach to self-supervised learning. *Advances in neural information processing systems*, 33:21271–21284, 2020.
- [20] Kaiming He, Xinlei Chen, Saining Xie, Yanghao Li, Piotr Dollár, and Ross Girshick. Masked autoencoders are scalable vision learners. In *Proceedings of the IEEE/CVF Conference on Computer Vision and Pattern Recognition*, pages 16000–16009, 2022.
- [21] Kaiming He, Haoqi Fan, Yuxin Wu, Saining Xie, and Ross Girshick. Momentum contrast for unsupervised visual representation learning. In *Proceedings of the IEEE/CVF conference on computer vision and pattern recognition*, pages 9729–9738, 2020.
- [22] Kaiming He, Georgia Gkioxari, Piotr Dollár, and Ross Girshick. Mask r-cnn. In *Proceedings of the IEEE international conference on computer vision*, pages 2961–2969, 2017.
- [23] Kaiming He, Xiangyu Zhang, Shaoqing Ren, and Jian Sun. Deep residual learning for image recognition. In *Proceedings of the IEEE conference on computer vision and pattern recognition*, pages 770–778, 2016.
- [24] R Devon Hjelm, Alex Fedorov, Samuel Lavoie-Marchildon, Karan Grewal, Phil Bachman, Adam Trischler, and Yoshua Bengio. Learning deep representations by mutual information estimation and maximization. *arXiv preprint arXiv:1808.06670*, 2018.
- [25] Sebastian Houben, Johannes Stallkamp, Jan Salmen, Marc Schlipsing, and Christian Igel. Detection of traffic signs in real-world images: The german traffic sign detection benchmark. In *The 2013 international joint conference on neural networks (IJCNN)*, pages 1–8. Ieee, 2013.
- [26] Phillip Isola, Daniel Zoran, Dilip Krishnan, and Edward H Adelson. Learning visual groups from co-occurrences in space and time. *arXiv preprint arXiv:1511.06811*, 2015.
- [27] Diederik P Kingma and Jimmy Ba. Adam: A method for stochastic optimization. *arXiv preprint arXiv:1412.6980*, 2014.
- [28] Diederik P Kingma and Max Welling. Auto-encoding variational bayes. *arXiv preprint arXiv:1312.6114*, 2013.
- [29] Lingpeng Kong, Cyprien de Masson d’Autume, Wang Ling, Lei Yu, Zihang Dai, and Dani Yogatama. A mutual information maximization perspective of language representation learning. 2020.

- [30] Alex Krizhevsky, Geoffrey Hinton, et al. Learning multiple layers of features from tiny images. 2009.
- [31] Gustav Larsson, Michael Maire, and Gregory Shakhnarovich. Learning representations for automatic colorization. In *Computer Vision–ECCV 2016: 14th European Conference, Amsterdam, The Netherlands, October 11–14, 2016, Proceedings, Part IV 14*, pages 577–593. Springer, 2016.
- [32] Yann LeCun, Léon Bottou, Yoshua Bengio, and Patrick Haffner. Gradient-based learning applied to document recognition. *Proceedings of the IEEE*, 86(11):2278–2324, 1998.
- [33] Tsung-Yi Lin, Michael Maire, Serge Belongie, James Hays, Pietro Perona, Deva Ramanan, Piotr Dollár, and C Lawrence Zitnick. Microsoft coco: Common objects in context. In *Computer Vision–ECCV 2014: 13th European Conference, Zurich, Switzerland, September 6–12, 2014, Proceedings, Part V 13*, pages 740–755. Springer, 2014.
- [34] Lajanugen Logeswaran and Honglak Lee. An efficient framework for learning sentence representations. 2018.
- [35] Antoine Miech, Jean-Baptiste Alayrac, Lucas Smaira, Ivan Laptev, Josef Sivic, and Andrew Zisserman. End-to-end learning of visual representations from uncurated instructional videos. In *Proceedings of the IEEE/CVF Conference on Computer Vision and Pattern Recognition*, pages 9879–9889, 2020.
- [36] Ishan Misra and Laurens van der Maaten. Self-supervised learning of pretext-invariant representations. In *Proceedings of the IEEE/CVF Conference on Computer Vision and Pattern Recognition*, pages 6707–6717, 2020.
- [37] Maria-Elena Nilsback and Andrew Zisserman. Automated flower classification over a large number of classes. In *2008 Sixth Indian Conference on Computer Vision, Graphics & Image Processing*, pages 722–729. IEEE, 2008.
- [38] Mehdi Noroozi and Paolo Favaro. Unsupervised learning of visual representations by solving jigsaw puzzles. In *European conference on computer vision*, pages 69–84, 2016.
- [39] Aaron van den Oord, Yazhe Li, and Oriol Vinyals. Representation learning with contrastive predictive coding. *arXiv preprint arXiv:1807.03748*, 2018.
- [40] Deepak Pathak, Philipp Krahenbuhl, Jeff Donahue, Trevor Darrell, and Alexei A Efros. Context encoders: Feature learning by inpainting. In *Proceedings of the IEEE conference on computer vision and pattern recognition*, pages 2536–2544, 2016.
- [41] Alec Radford, Jong Wook Kim, Chris Hallacy, Aditya Ramesh, Gabriel Goh, Sandhini Agarwal, Girish Sastry, Amanda Askell, Pamela Mishkin, Jack Clark, et al. Learning transferable visual models from natural language supervision. In *International conference on machine learning*, pages 8748–8763. PMLR, 2021.
- [42] Shaoqing Ren, Kaiming He, Ross Girshick, and Jian Sun. Faster r-cnn: Towards real-time object detection with region proposal networks. *Advances in neural information processing systems*, 28, 2015.
- [43] Pierre Sermanet, Corey Lynch, Yevgen Chebotar, Jasmine Hsu, Eric Jang, Stefan Schaal, Sergey Levine, and Google Brain. Time-contrastive networks: Self-supervised learning from video. In *2018 IEEE international conference on robotics and automation (ICRA)*, pages 1134–1141, 2018.
- [44] Stefano Soatto and Alessandro Chiuso. Visual representations: Defining properties and deep approximations. In *ICLR*, 2016.
- [45] Karthik Sridharan and Sham M Kakade. An information theoretic framework for multi-view learning. 2008.
- [46] Aravind Srinivas, Michael Laskin, and Pieter Abbeel. Curl: Contrastive unsupervised representations for reinforcement learning. *arXiv preprint arXiv:2004.04136*, 2020.
- [47] Yixuan Su, Tian Lan, Yan Wang, Dani Yogatama, Lingpeng Kong, and Nigel Collier. A contrastive framework for neural text generation. *arXiv preprint arXiv:2202.06417*, 2022.
- [48] Chen Sun, Fabien Baradel, Kevin Murphy, and Cordelia Schmid. Learning video representations using contrastive bidirectional transformer. *arXiv preprint arXiv:1906.05743*, 2019.
- [49] Yonglong Tian, Dilip Krishnan, and Phillip Isola. Contrastive multiview coding. In *ECCV*, 2020.
- [50] Yonglong Tian, Chen Sun, Ben Poole, Dilip Krishnan, Cordelia Schmid, and Phillip Isola. What makes for good views for contrastive learning? *Advances in Neural Information Processing Systems*, 33:6827–6839, 2020.
- [51] Naftali Tishby, Fernando C. Pereira, and William Bialek. The information bottleneck method. In *Proc. of the 37-th Annual Allerton Conference on Communication, Control and Computing*, pages 368–377, 1999.
- [52] Yao-Hung Hubert Tsai, Yue Wu, Ruslan Salakhutdinov, and Louis-Philippe Morency. Self-supervised learning from a multi-view perspective. *arXiv preprint arXiv:2006.05576*, 2020.
- [53] Michael Tschannen, Josip Djolonga, Paul K Rubenstein, Sylvain Gelly, and Mario Lucic. On mutual information maximization for representation learning. *arXiv preprint arXiv:1907.13625*, 2019.
- [54] Catherine Wah, Steve Branson, Peter Welinder, Pietro Perona, and Serge Belongie. The caltech-ucsd birds-200-2011 dataset. 2011.
- [55] Haoqing Wang, Xun Guo, Zhi-Hong Deng, and Yan Lu. Rethinking minimal sufficient representation in contrastive learning. In *Proceedings of the IEEE/CVF Conference on Computer Vision and Pattern Recognition*, pages 16041–16050, 2022.
- [56] Zhirong Wu, Yuanjun Xiong, Stella X Yu, and Dahua Lin. Unsupervised feature learning via non-parametric instance discrimination. In *Proceedings of the IEEE conference on computer vision and pattern recognition*, 2018.
- [57] Han Xiao, Kashif Rasul, and Roland Vollgraf. Fashion-mnist: a novel image dataset for benchmarking machine learning algorithms. *arXiv preprint arXiv:1708.07747*, 2017.
- [58] Chang Xu, Dacheng Tao, and Chao Xu. A survey on multi-view learning. *arXiv preprint arXiv:1304.5634*, 2013.
- [59] Jiarui Xu and Xiaolong Wang. Rethinking self-supervised correspondence learning: A video frame-level similarity perspective. In *Proceedings of the IEEE/CVF International Conference on Computer Vision*, pages 10075–10085, 2021.

- [60] Zhilin Yang, Zihang Dai, Yiming Yang, Jaime Carbonell, Russ R Salakhutdinov, and Quoc V Le. Xlnet: Generalized autoregressive pretraining for language understanding. *Advances in neural information processing systems*, 32, 2019.
- [61] Mang Ye, Xu Zhang, Pong C Yuen, and Shih-Fu Chang. Unsupervised embedding learning via invariant and spreading instance feature. In *Proceedings of the IEEE/CVF Conference on Computer Vision and Pattern Recognition*, pages 6210–6219, 2019.
- [62] Yang You, Igor Gitman, and Boris Ginsburg. Scaling sgd batch size to 32k for imagenet training. *arXiv preprint arXiv:1708.03888*, 6(12):6, 2017.
- [63] Yun Yue, Fangzhou Lin, Kazunori D Yamada, and Ziming Zhang. Hyperbolic contrastive learning. *arXiv preprint arXiv:2302.01409*, 2023.
- [64] Jure Zbontar, Li Jing, Ishan Misra, Yann LeCun, and Stéphane Deny. Barlow twins: Self-supervised learning via redundancy reduction. In *International Conference on Machine Learning*, pages 12310–12320. PMLR, 2021.
- [65] Dejiao Zhang, Feng Nan, Xiaokai Wei, Shangwen Li, Henghui Zhu, Kathleen McKeown, Ramesh Nallapati, Andrew Arnold, and Bing Xiang. Supporting clustering with contrastive learning. *arXiv preprint arXiv:2103.12953*, 2021.
- [66] Liheng Zhang, Guo-Jun Qi, Liqiang Wang, and Jiebo Luo. Aet vs. aed: Unsupervised representation learning by auto-encoding transformations rather than data. In *Proceedings of the IEEE/CVF Conference on Computer Vision and Pattern Recognition*, pages 2547–2555, 2019.
- [67] Richard Zhang, Phillip Isola, and Alexei A Efros. Colorful image colorization. In *Computer Vision—ECCV 2016: 14th European Conference, Amsterdam, The Netherlands, October 11–14, 2016, Proceedings, Part III 14*, pages 649–666. Springer, 2016.
- [68] Richard Zhang, Phillip Isola, and Alexei A Efros. Split-brain autoencoders: Unsupervised learning by cross-channel prediction. In *Proceedings of the IEEE conference on computer vision and pattern recognition*, pages 1058–1067, 2017.
- [69] Nanxuan Zhao, Zhirong Wu, Rynson WH Lau, and Stephen Lin. Distilling localization for self-supervised representation learning. In *Proceedings of the AAAI Conference on Artificial Intelligence*, volume 35, pages 10990–10998, 2021.
- [70] Chengxu Zhuang, Tianwei She, Alex Andonian, Max Sobol Mark, and Daniel Yamins. Unsupervised learning from video with deep neural embeddings. In *Proceedings of the IEEE/CVF Conference on Computer Vision and Pattern Recognition*, pages 9563–9572, 2020.
- [71] Chengxu Zhuang, Alex Lin Zhai, and Daniel Yamins. Local aggregation for unsupervised learning of visual embeddings. In *Proceedings of the IEEE/CVF International Conference on Computer Vision*, pages 6002–6012, 2019.

A. Properties of Mutual Information

In this section we list some properties [9] of mutual information and use these properties to prove theorems and equations in this paper. For any random variables \mathbf{x} , \mathbf{y} and \mathbf{z} , the following equations hold.

(P₁) Symmetry:

$$I(\mathbf{x}; \mathbf{y}) = I(\mathbf{y}; \mathbf{x})$$

(P₂) Non-negativity:

$$I(\mathbf{x}; \mathbf{y}) \geq 0, I(\mathbf{x}; \mathbf{y}|\mathbf{z}) \geq 0$$

(P₃) Chain rule:

$$I(\mathbf{x}, \mathbf{y}; \mathbf{z}) = I(\mathbf{y}; \mathbf{z}) + I(\mathbf{x}; \mathbf{z}|\mathbf{y})$$

(P₄) Multivariate Mutual Information:

$$I(\mathbf{x}; \mathbf{y}; \mathbf{z}) = I(\mathbf{y}; \mathbf{z}) - I(\mathbf{y}; \mathbf{z}|\mathbf{x})$$

B. Proofs

Before the detailed derivation, we have the following assumption, if a random variable \mathbf{z} is defined to be a representation of another random variable \mathbf{x} , we state that \mathbf{z} is conditionally independent from any other variable in the model once \mathbf{z} is observed. This assumption is also reported in [16].

$$I(\mathbf{z}; \mathbf{a}|\mathbf{x}, \mathbf{b}) = 0$$

where \mathbf{a} and \mathbf{b} represent any other variable (or groups of variables) in supervised and self-supervised settings.

B.1. Proof of Equation 1

Equation 1: $I(\mathbf{x}; \mathbf{z})$ can be decomposed into two terms, $I(\mathbf{x}; \mathbf{z}) = I(\mathbf{y}; \mathbf{z}) + I(\mathbf{x}; \mathbf{z}|\mathbf{y})$.

Proof. Using Property 3 in Appendix A, we see that

$$I(\mathbf{x}, \mathbf{y}; \mathbf{z}) = I(\mathbf{y}; \mathbf{z}) + I(\mathbf{x}; \mathbf{z}|\mathbf{y})$$

at the same time, by changing the order of \mathbf{x} and \mathbf{y} , we also have that

$$I(\mathbf{x}, \mathbf{y}; \mathbf{z}) = I(\mathbf{x}; \mathbf{z}) + I(\mathbf{y}; \mathbf{z}|\mathbf{x})$$

Based on the assumption above, $I(\mathbf{y}; \mathbf{z}|\mathbf{x}) = 0$, so $I(\mathbf{x}; \mathbf{z}) = I(\mathbf{y}; \mathbf{z}) + I(\mathbf{x}; \mathbf{z}|\mathbf{y})$, Equation 1 holds. \square

B.2. Proof of Equation 2

Equation 2: $I(\mathbf{v}_1; \mathbf{z}_1)$ can be decomposed into two terms, $I(\mathbf{v}_1; \mathbf{z}_1) = I(\mathbf{v}_2; \mathbf{z}_1) + I(\mathbf{v}_1; \mathbf{z}_1|\mathbf{v}_2)$.

Proof. Using Property 4, we see that

$$I(\mathbf{v}_1; \mathbf{z}_1) = I(\mathbf{v}_1; \mathbf{z}_1|\mathbf{v}_2) + I(\mathbf{v}_2; \mathbf{v}_1; \mathbf{z}_1)$$

Using Property 4 again, we have that

$$I(\mathbf{v}_2; \mathbf{v}_1; \mathbf{z}_1) = I(\mathbf{v}_2; \mathbf{z}_1) - I(\mathbf{v}_2; \mathbf{z}_1|\mathbf{v}_1)$$

According to the assumption above, $I(\mathbf{v}_2; \mathbf{z}_1|\mathbf{v}_1) = 0$, so $I(\mathbf{v}_1; \mathbf{z}_1) = I(\mathbf{v}_2; \mathbf{z}_1) + I(\mathbf{v}_1; \mathbf{z}_1|\mathbf{v}_2)$, Equation 2 holds. \square

C. Implementation of the objective function

C.1. Implementation of $I(\mathbf{v}_i; \mathbf{z}_i)$ ($i = 1, 2$)

We first expand the $I(\mathbf{v}_i; \mathbf{z}_i)$ by the definition of mutual information and then apply several operations. Assuming $r(\mathbf{z}_i)$ is a variational approximation to this marginal, and because of $p(\mathbf{z}_i) = \int d\mathbf{v}_i p(\mathbf{z}_i|\mathbf{v}_i)p(\mathbf{v}_i)$ and $\mathbf{KL}[p(\mathbf{z}_i), r(\mathbf{z}_i)] \geq 0$, we have that

$$\begin{aligned} I(\mathbf{v}_i; \mathbf{z}_i) &= \iint d\mathbf{v}_i d\mathbf{z}_i p(\mathbf{v}_i)p(\mathbf{z}_i|\mathbf{v}_i) \log \frac{p(\mathbf{z}_i|\mathbf{v}_i)}{p(\mathbf{z}_i)} \\ &= \iint d\mathbf{v}_i d\mathbf{z}_i p(\mathbf{v}_i)p(\mathbf{z}_i|\mathbf{v}_i) \log \frac{p(\mathbf{z}_i|\mathbf{v}_i)}{r(\mathbf{z}_i)} \\ &\quad - \iint d\mathbf{v}_i d\mathbf{z}_i p(\mathbf{v}_i)p(\mathbf{z}_i|\mathbf{v}_i) \log \frac{p(\mathbf{z}_i)}{r(\mathbf{z}_i)} \\ &= \iint d\mathbf{v}_i d\mathbf{z}_i p(\mathbf{v}_i, \mathbf{z}_i) \log \frac{p(\mathbf{z}_i|\mathbf{v}_i)}{r(\mathbf{z}_i)} \\ &\quad - \int d\mathbf{z}_i p(\mathbf{z}_i) \log \frac{p(\mathbf{z}_i)}{r(\mathbf{z}_i)} \\ &= \iint d\mathbf{v}_i d\mathbf{z}_i p(\mathbf{v}_i, \mathbf{z}_i) \log \frac{p(\mathbf{z}_i|\mathbf{v}_i)}{r(\mathbf{z}_i)} \\ &\quad - \mathbf{KL}[p(\mathbf{z}_i), r(\mathbf{z}_i)] \\ &\leq \iint d\mathbf{v}_i d\mathbf{z}_i p(\mathbf{v}_i, \mathbf{z}_i) \log \frac{p(\mathbf{z}_i|\mathbf{v}_i)}{r(\mathbf{z}_i)} \\ &= \mathbf{KL}[p(\mathbf{z}_i|\mathbf{v}_i), r(\mathbf{z}_i)] \end{aligned}$$

Further we assume the encoder process follows the Gaussian distribution, $p(\mathbf{z}_i|\mathbf{v}_i) = \mathcal{N}(\mathbf{z}_i; f_i(\mathbf{v}_i), \sigma_i^2 I)$ and the variational approximation $r(\mathbf{z}_i) = \mathcal{N}(\mathbf{0}, I)$, so the following equation holds, d is the of embedding vectors.

$$\mathbf{KL}[p(\mathbf{z}_i|\mathbf{v}_i), r(\mathbf{z}_i)] = -\frac{1}{2} \sum_{i=1}^d (1 + \log(\sigma_i^2) - f_i^2(\mathbf{v}_i) - \sigma_i^2)$$

According the above expression, it can be conveniently implemented with code.

C.2. Implementation of $I(\mathbf{v}_1; \mathbf{z}_2)$, $I(\mathbf{v}_2; \mathbf{z}_1)$

On the other hand, we need the lower bound of the positive terms $I(\mathbf{v}_1; \mathbf{z}_2)$ and $I(\mathbf{v}_2; \mathbf{z}_1)$, take $I(\mathbf{v}_1; \mathbf{z}_2)$ as the example. Assuming $q(\mathbf{v}_1|\mathbf{z}_2)$ is the variational approximation to $p(\mathbf{v}_1|\mathbf{z}_2)$ in order to deal with the intractability of this conditional distribution, we have the following proof.

$$\begin{aligned}
I(\mathbf{v}_1; \mathbf{z}_2) &= \iint d\mathbf{v}_1 d\mathbf{z}_2 p(\mathbf{v}_1, \mathbf{z}_2) \log \frac{p(\mathbf{v}_1|\mathbf{z}_2)}{p(\mathbf{v}_1)} \\
&= \iint d\mathbf{v}_1 d\mathbf{z}_2 p(\mathbf{v}_1, \mathbf{z}_2) \log p(\mathbf{v}_1|\mathbf{z}_2) \\
&\quad - \iint d\mathbf{v}_1 d\mathbf{z}_2 p(\mathbf{v}_1, \mathbf{z}_2) \log p(\mathbf{v}_1) \\
&\approx \iint d\mathbf{v}_1 d\mathbf{z}_2 p(\mathbf{v}_1, \mathbf{z}_2) \log q(\mathbf{v}_1|\mathbf{z}_2) + H(\mathbf{v}_1) \\
&= \mathbb{E}_{p(\mathbf{v}_1, \mathbf{z}_2)}[\log q(\mathbf{v}_1|\mathbf{z}_2)] + H(\mathbf{v}_1)
\end{aligned}$$

Where $H(\mathbf{v}_1)$ is a constant given the augmentation view during objective optimization, so it is equivalent to maximize $\mathbb{E}_{p(\mathbf{v}_1, \mathbf{z}_2)}[\log p(\mathbf{v}_1|\mathbf{z}_2)]$. Further we suppose $q(\mathbf{v}_1|\mathbf{z}_2) = \mathcal{N}(\mathbf{v}_1; h_1(\mathbf{z}_2), \sigma_3^2 I)$, where h_1 maps \mathbf{z}_2 to \mathbf{v}_1 which we can use an compact **deConvNet** for realization, thus, we are able to estimate and implement $\mathbb{E}_{p(\mathbf{v}_1, \mathbf{z}_2)}[\log q(\mathbf{v}_1|\mathbf{z}_2)]$. (similar to $I(\mathbf{v}_2; \mathbf{z}_1)$).

$$\mathbb{E}_{p(\mathbf{v}_1, \mathbf{z}_2)}[\log q(\mathbf{v}_1|\mathbf{z}_2)] \propto -\mathbb{E}_{p(\mathbf{v}_1, \mathbf{z}_2)}[\|\mathbf{v}_1 - h_1(\mathbf{z}_2)\|_2^2] + c$$

where c is a constant to representation \mathbf{z}_2 .

Based on these derivations, we can implement the final loss function L

$$\begin{aligned}
L &= -I(\mathbf{z}_1; \mathbf{z}_2) + \sum_{i=1}^2 \lambda_i \mathbf{KL}[p(\mathbf{z}_i|\mathbf{v}_i), r(\mathbf{z}_i)] \\
&\quad - \lambda_3 \mathbb{E}_{p(\mathbf{v}_1, \mathbf{z}_2)}[\log q(\mathbf{v}_1|\mathbf{z}_2)] - \lambda_4 \mathbb{E}_{p(\mathbf{v}_2, \mathbf{z}_1)}[\log q(\mathbf{v}_2|\mathbf{z}_1)]
\end{aligned}$$